arXiv:1410.6418v1 [nucl-ex] 23 Oct 2014

High-precision measurements of πp elastic differential cross sections in the second resonance region

I. G. Alekseev[1], V. A. Andreev[3], I. G. Bordyuzhin[1,5], W. J. Briscoe[2], Ye. A. Filimonov[3], V. V. Golubev[3], A. B. Gridnev[3], D. V. Kalinkin[1], L. I. Koroleva[1], N. G. Kozlenko[3], V. S. Kozlov[3], A. G. Krivshich[3], B. V. Morozov[1], V. M. Nesterov[1], D. V. Novinsky[3], V. V. Ryltsov[1], M. Sadler[4], B.M. Shurygin[1], I. I. Strakovsky[2], A. D. Sulimov[1], V. V. Sumachev[3], D. N. Svirida[1], V. I. Tarakanov[3], V. Yu. Trautman[3], R. L. Workman[2]

(EPECUR Collaboration and GW INS Data Analysis Center)

[1] *Institute for Theoretical and Experimental Physics, Moscow, 117218, Russia*
[2] *The George Washington University, Washington, DC 20052, USA*
[3] *Petersburg Nuclear Physics Institute, Gatchina, 188300, Russia*
[4] *Abilene Christian University, Abilene, Texas, TX 79699-7963, USA and*
[5] *National University of Science and Technology "MISiS", Moscow, 119049, Russia*

(Dated: October 24, 2014)

Cross sections for $\pi^{\pm}p$ elastic scattering have been measured to high precision, for beam momenta between 800 and 1240 MeV/c, by the EPECUR Collaboration, using the ITEP proton synchrotron. The data precision allows comparisons of the existing partial-wave analyses (PWA) on a level not possible previously. These comparisons imply that updated PWA are required.

PACS numbers: 12.40.Vv,13.60.Le,14.40.Be,25.20.Lj

Measurements of πp elastic differential cross sections by the EPECUR group, at the ITEP 10 GeV proton synchrotron, have produced data of unprecedented precision for beam momenta from 800 to 1240 MeV/c (2638 π^+p and 4277 π^-p data points). This energy range, which covers center-of-mass energies from 1560 to 1800 MeV, was motivated by the search for a narrow structure associated with the pentaquark anti-decuplet [1], expected near 1.7 GeV.

The data precision required to search for such a narrow structure has produced cross sections capable of identifying both narrow resonance-like signals and cusps expected to appear at the thresholds of opening production channels, such as $K\Lambda$ and $K\Sigma$. The precision also greatly exceeds that of previously available cross sections, which were used to generate the Karlsruhe-Helsinki [2] (KH) and Carnegie-Mellon-Berkeley [3] (CMB) fits, from which much of non-strange baryon spectrum was determined. This allows a comparison of the classical KH and CMB analyses, and the more recent GW results [4], at a level not possible with the existing database.

Below, we first describe the experimental design and analysis. We then outline cases where a clear distinction exists between the new data and some of these older analyses.

The layout of the experiment [5] is shown in Fig. 1. This is a two-arm non-magnetic spectrometer placed in the second focus of a universal high resolution secondary beam line of the ITEP proton synchrotron. The first focus of the beam line is equipped by a set of four 2-coordinate proportional chambers (**1FCH1-4** in Fig. 1) with 1 mm pitch, which allow the tagging of each beam particle with its momentum with the precision about 0.1%. Similar set of proportional chambers (**2FCH1-4**) is placed in the second focus in front of the target. Beam size (σ) at the target is 5.5 mm and 3.5 mm in the horizontal and vertical planes correspondingly. "Magic" (argon-isobutane-freon) gas mixture is used in proportional chambers. Beam tests showed better than 99% efficiency. The liquid hydrogen reservoir of the target is made of mylar and has 40 mm in diameter and about 250 mm in length along the beam. The reservoir is placed in a vacuum-tight 80 mm diameter beryllium outer shell with a mylar covered window on the beam entrance flange. Scattered particles are measured by two symmetrical arms of drift chambers (**DC1-8**) with hexagonal structure. Each arm consists of 4 chambers. Wires in odd-numbered chambers are horizontal, with even-numbered wires being vertical. Each chamber has 2 sensitive wire planes with a 17 mm pitch. The planes are shifted by half of the pitch. The two chambers closest to the target have a sensitive area 600×400 mm^2. Six other chambers have sensitive area 1200×800 mm^2. A gas mixture of 70% Ar and 30% CO_2 is used in the drift chambers. Beam tests showed better than 99% single drift plane efficiency with 0.2 mm resolution for perpendicular tracks.

Central beam momentum was calibrated with 0.1% precision at three values: 1057, 1095, and 1297 MeV/c using protons of the internal accelerator beam elastically scattered on the beryllium target. The field of the last dipole magnet of the beam line is controlled by NMR, providing stability of the energy calibration. In addition to the pions, the beam contains also electrons (positrons), muons and protons (for the positive beam). Contamination from other particles (kaons and anti-protons) is negligible. Protons were rejected at the trigger level by time of flight between scintillator counters in the first and the second focuses. The residual proton contamination was checked using the difference between pp and

πp elastic kinematics and was found to be less than 0.2%. The contribution of electrons and muons was measured using gas Cherenkov counter and simulated using Geant4 [6]. The fraction of electrons (positrons) is about 3% at 840 MeV/c falling approximately linear to 1.5% at 1240 MeV/c and the fraction of muons falls in this range from 6% to 4%.

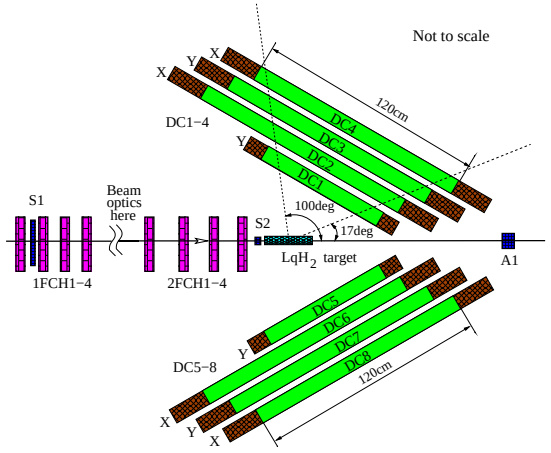

FIG. 1. (Color on-line) The experimental setup (top view). **1FCH1-4** and **2FCH1-4** — 1-mm pitch proportional chambers, **DC1-DC8** — drift chambers, **LH$_2$** — liquid hydrogen target, **S1**, **S2** and **A1** — trigger scintillation counters.

A unique distributed DAQ system, based on the commercial 480 Mbit/s USB 2.0 interface, was designed for the experiment [7]. It consists of 100-channel boards for proportional chambers and 24-channel boards for drift chambers, placed on the chamber frames. Trigger logic is capable of processing several trigger conditions activating different sets of detectors. DAQ features nearly dead-time-less operation and can process up to 10^5 events per spill. A soft trigger condition was used to acquire physics events:

$$T = S_1 \cdot S_2 \cdot M_{1FCH} \cdot M_{2FCH} \cdot \overline{A_1}, \qquad (1)$$

where S_1, S_2, and A_1 are signals from corresponding scintillation counters and M_{1FCH} and M_{2FCH} are fast signals from the proportional chamber blocks in the 1$^{\text{st}}$ and the 2$^{\text{nd}}$ focuses. Other trigger conditions with large prescale were used for beam position and luminosity monitoring. During data taking the momentum range was scanned with 15 MeV/c steps in the central momentum of the beam, which is about one half of the momentum spread in each step.

Selection of the elastic events in this experiment is based on the angular correlation of pion and proton tracks. A single track is required in the beam chambers and both scattering arms. All of these tracks are required to form a common vertex inside the target and lie in a plane. A central of mass scattering angle θ_{CM} is calculated for both scattered particles under the assumption that the pion has scattered to the left. A distribution of the events over the difference between reconstructed scattering angles $\Delta\theta_{CM}$ and the scattering angle θ_{CM} is shown in Fig. 2a for one beam momentum setting. Two clusters are clearly seen. One corresponds to the pion scattered to the left (the assumption was correct) and the other corresponds to the pion scattered to the right (the assumption was wrong). A slice of the distribution for a one degree θ_{CM} interval $\theta_{CM} = 84°$ is shown in Fig. 2b. This figure also illustrates the amount of inelastic background, which was calculated and subtracted in each bin. Differential cross sections were calculated from the number of elastic events corrected for acceptance and chamber efficiency. Beam monitor is based on a special trigger, which ignores counter A_1, used as a veto in the main trigger. Numeric characteristics of the data sample are presented in Table I.

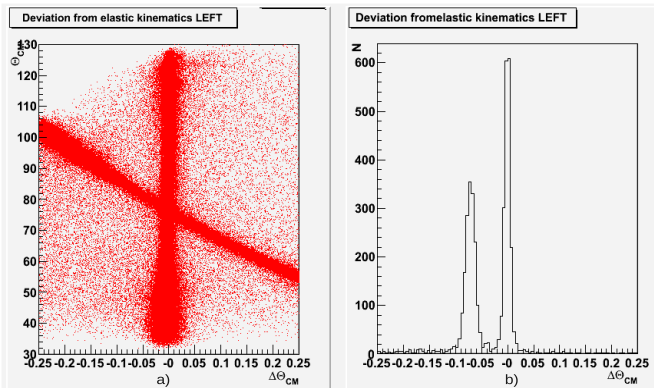

FIG. 2. (Color on-line) 2-dimensional distribution over the difference between calculated center of mass scattering angles for pion and proton, assuming that the pion goes to the left arm, $\Delta\theta_{CM}$ (abscissa) and the scattering angle θ_{CM} (ordinate) - (a) and its slice at $\theta_{CM} = 84°$ (b).

TABLE I. Parameters of the statistics presented

	$\pi^- p \to \pi^- p$	$\pi^+ p \to \pi^+ p$
θ_{CM} angle range (°)	$40 - 122$	$40 - 122$
Beam momentum range (GeV/c)	$0.80 - 1.24$	$0.92 - 1.24$
Triggers accumulated	$1.25 \cdot 10^9$	$0.69 \cdot 10^9$
Elastic events	$2.24 \cdot 10^7$	$1.48 \cdot 10^7$

Main systematic error contributions are listed in Table II. We estimate total systematic uncertainty as sum in quadratures of the uncertanties in the table as 2.6%.

In order to search for a narrow structure, data with a fine energy grid and high precision are required, and have been achieved. These cross sections have placed far higher constraints on existing partial-wave analysis (PWA) than any previous experiment. As a result, angular structures are extremely well defined and clearly differentiate between the classic analyses of the KH [2], CMB [3], and GW DAC [4] groups. Their inclusion in

TABLE II. Systematic errors

Systematic error origin	Base for the estimation	Error
Beam pollution with electrons and muons	Comparison between Monte-Carlo and Cherenkov counter measurements	1%
Luminocity normalization	Comparison of elastic events yield for all angles in the overlapping momentum ranges	2%
Tracking efficiency and setup geometry	Comparison between cross sections obtained for events with pion hitting the left arm to those with pion hitting the right arm	1%
Monte-Carlo simulations of the acceptance	Comparison between two independent acceptance simulations used	0.8%
Various cuts used in the analysis	Dependence of the event yield from the cut	0.5%

future PWA will help to discriminate between competing mechanisms for sharp structures, such as the proposed antidecuplet, S-P wave resonance interference [8], or possible threshold cusp effects [9].

In Fig. 3, we plot fixed-angle cross sections near 90 degrees and compare with both the older datasets and the prediction based on fits to these older data. The higher precision now available can, in some cases, clearly select the older CMB and recent GW DAC fits over the KH fit (KA84). The earlier KH fit, KH80 [2], fares somewhat better in these comparisons. Evidence for a possible sharp structure at more forward angles, near both a possible N(1685) resonance and the $K\Sigma$ threshold has been reported previously [11]. Such structures are not evident in any existing fit. The resonance hypothesis has also been tested in the fit of Ref. [12].

In Fig. 4, we plot several angular distributions to give an alternate view of the fits/predictions versus data. From the left and central panel, we see how similar the existing predictions are, in general, with differences magnified in the view of Fig. 3. In the right panel, the KA84 fit is compared to a preliminary GW DAC fit to the new data. The GW fit employs a searchable renormalization factor, which gives a chi-squared penalty determined by the overall systematic error [4]. In this case, as opposed to the other energies displayed in Fig. 4, the renormalization produces a good description of the data, but is rather large compared to the systematic uncertainty, suggesting a more detailed analysis may be required. A more careful analysis could involve multi-channel fits with analytically built-in thresholds for opening channels. Work in this direction is planned, based on the Jülich model of pion-induced reactions [9].

The authors wish to acknowledge the excellent support of the accelerator group and operators of ITEP. This work was partially supported by Russian Fund for Basic Research grants 09-02-00998a and 05-02-17005a and by the U.S. Department of Energy, Office of Science, Office of Nuclear Physics, under Award Number DE.FG02.99ER41110.

[1] D. I. Diakonov, V. Yu. Petrov, and M. V. Polyakov, Z. F. Physik A **359**, 305 (1997); R. A. Arndt *et al.*, Phys. Rev. C **69**, 035208 (2004).
[2] G. Höhler, *Pion Nucleon Scattering*, Part 2, Landolt-Bornstein, Vol.9b, 1983.
[3] R. E. Cutkosky *et al.*, Phys. Rev. D **20**, 2839 (1979); R. E. Cutkosky in *Proceedings of the 4th Conference on Baryon Resonances*, ed. N. Isgur, (Toronto, 1983).
[4] R. L. Workman, R. A. Arndt, W. J. Briscoe, M. W. Paris, I.I. Strakovsky, Phys. Rev. C **86**, 035202 (2012); R. A. Arndt, W. J. Briscoe, I. I. Strakovsky, and R. L. Workman, Phys. Rev. C **74**, 045205 (2006).
[5] I. G. Alekseev *et al.*, Instrum. Exp. Tech. **57**, 535 (2014); I. G. Alekseev *et al.*, arXiv:0509032 [hep-ex].
[6] S. Agostinelli *et al.* (Geant4 Collaboration), Nucl. Instrum. Meth. A **506** 250 (2003); http://geant4.cern.ch/
[7] I. G. Alekseev *et al.*, Nucl. Instrum. Meth. A **578** 289 (2007).
[8] V. Shklyar, H. Lenske, and U. Mosel, Phys. Rev. C **87**, 015201 (2013).
[9] M. Döring and K. Nakayama, Phys. Lett. B **683**, 145 (2010).
[10] R. Koch, Z. Phys. C **29**, 597 (1985).
[11] I.G. Alekseev et al, Int. J. Mod. Phys. Conf. Ser. **26**, 1460076 (2014).
[12] A. B. Gridnev, Proceedings of the XVth International Conference on Hadron Spectroscopy (Hadron 2013), Nara, Japan, Nov. 2013, Proceedings of Science (Hadron 2014) 099.

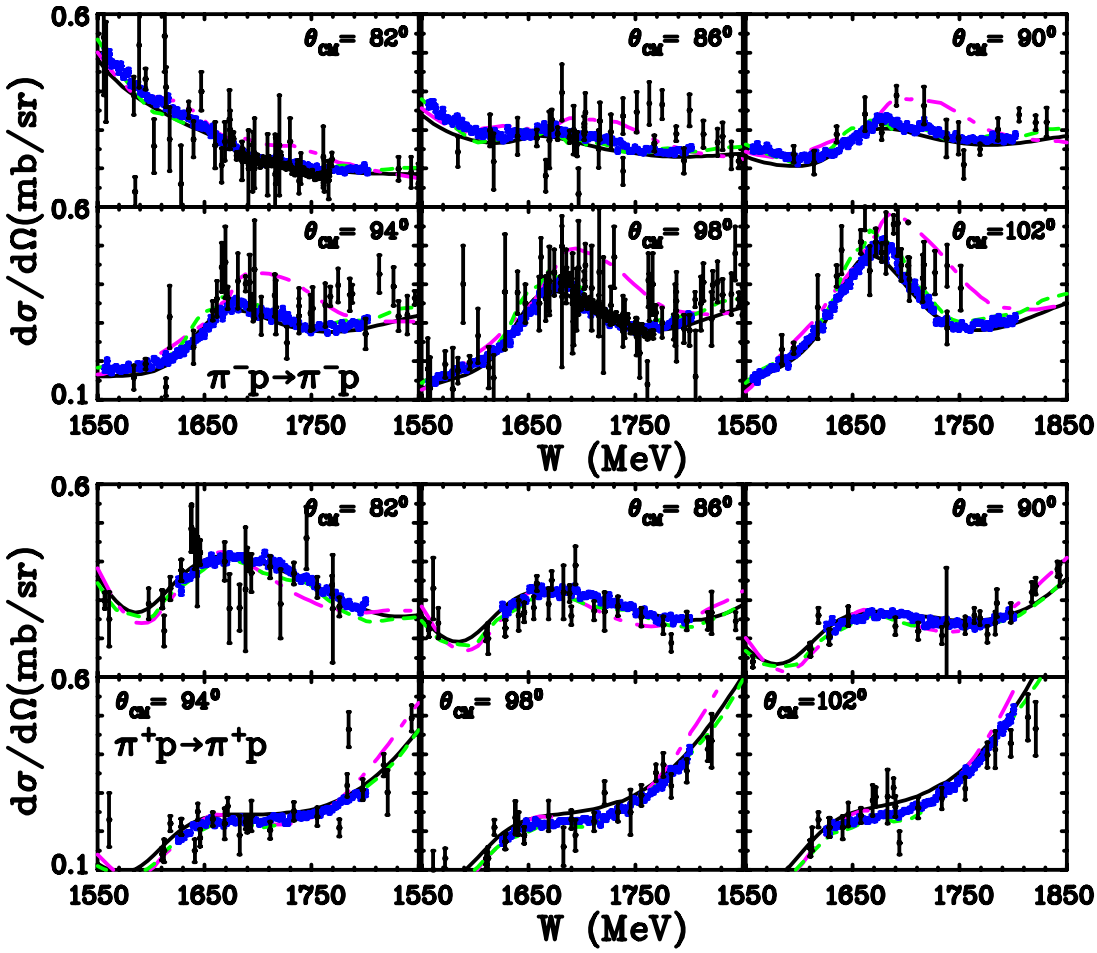

FIG. 3. (Color on-line) Excitation functions for selected angles around 90° in the center-of-mass frame, θ_{CM}, for $\pi^- p$ (top panel) and $\pi^+ p$ (bottom panel) elastic scattering. New EPECUR data (statistical errors only) are plotted as blue filled circles with previous measurements presented as black filled small circles. (The data from earlier experiments are within bins of $\Delta\theta_{CM} = \pm 1°$). An existing GW INS DAC fit, WI08 [4], is plotted with a solid black curve while the older KA84 [10] and CMB [3] fits are plotted as magenta dash-dotted and green dashed curves, respectively.

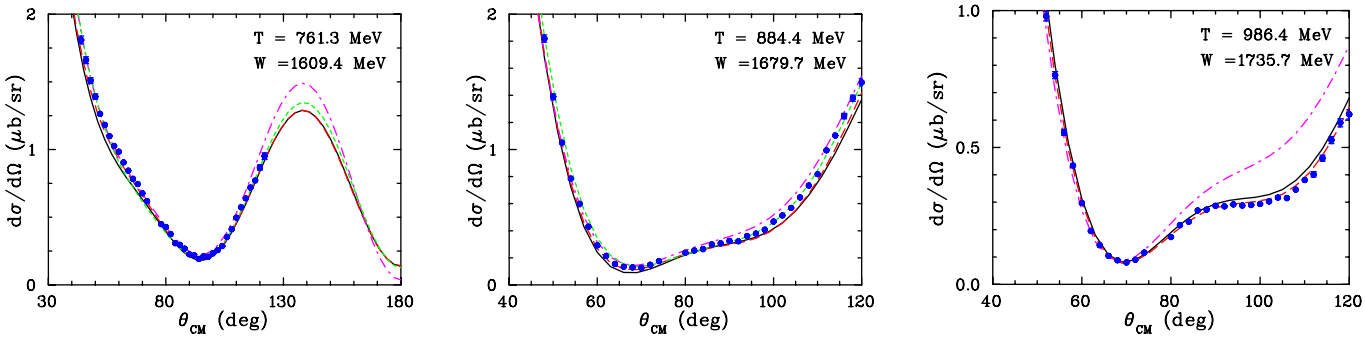

FIG. 4. (Color on-line) Differential cross sections for $\pi^- p$ elastic scattering, θ_{CM}, for selected energies. Left: T=761.3 MeV, middle: 884.4 MeV, and right: 986.4 MeV. New EPECUR data (statistical errors only) are plotted as blue filled circles. For left and middle panels, our recent prediction, WI08 [4], is plotted with black solid curves while the older KA84 [10] and CMB [3] fits are plotted as magenta dash-dotted and green dashed curves. For the right panel, exploratory fit WI14 (with and without normalization factor), including the new EPECUR data, is plotted with dashed red and black solid curves respectively, while the older KA84 [10] fit is plotted as a magenta dash-dotted curve for comparison.